(This is a sample cover image for this issue. The actual cover is not yet available at this time.)

Earth and Planetary Science Letters 364 (2013) 37–43

Contents lists available at SciVerse ScienceDirect

Earth and Planetary Science Letters

journal homepage: www.elsevier.com/locate/epsl

The incorporation of water into lower-mantle perovskites: A first-principles study

E.R. Hernández [a,*], D. Alfè [b], J. Brodholt [b,**]

[a] Instituto de Ciencia de Materials de Madrid (ICMM–CSIC), Campus de Cantoblanco, 28049 Madrid, Spain
[b] Department of Earth Sciences, University College London, Gower Street, London WC1E 6BT, United Kingdom

ARTICLE INFO

Article history:
Received 16 July 2012
Received in revised form
4 December 2012
Accepted 7 January 2013
Editor: T. Elliott

Keywords:
partition coefficient
water in mantle minerals
first principles simulation

ABSTRACT

We have used first principles methods to calculate the partitioning of water between perovskite and ringwoodite under lower mantle and Fe-free conditions. We find that incorporation of water into ringwoodite is more favourable than into perovskite by about 0.25 eV per formula unit, or about 24 kJ/mol. This translates to a ringwoodite to perovskite partition coefficient of between 10 and 13, depending on temperature. These values are in good agreement with the partitioning experiments of Inoue et al. (2010) on Fe-bearing samples, where they find a partition coefficient of about 15. We also find that water incorporates into perovskite more readily than into periclase (also under Fe-free conditions), and we predict a perovskite to periclase partition coefficient of 90 at 24 GPa and 1500 K. We conclude, therefore, that the lower-mantle is able to contain substantial amounts of water, perhaps as much as 1000 ppm.

1. Introduction

It has long been known that the nominally anhydrous transition zone minerals, wadsleyite and ringwoodite, can incorporate substantial amounts of water into their structure (Bell and Rossman, 1992; Smyth, 1994; Kohlstedt et al., 1996; Bolfan-Casanova, 2005). This has led to various models for how the dynamics and behaviour of upper mantle and transition zone may be affected by water, particularly through hydrolytic weakening and lowering of melting temperatures. Although the ability of the upper mantle and transition zone to incorporate large amounts of water is well accepted, the actual amount of water that the lower mantle is able to contain is still a matter of some debate. Some experimental studies conclude that perovskite can accommodate almost no water into its structure (Bolfan-Casanova et al., 2000, 2002), or perhaps a maximum of 100 ppm (Litasov et al., 2003), while others (Murakami et al., 2002; Inoue et al., 2010) have reported larger water uptake, ranging between 0.1 and 0.2 wt% (1000–2000 ppm).

It is currently not clear which results are correct. The apparent discrepancies between the available experimental reports can perhaps be explained in terms of the differing compositions employed in each study. Although all the experiments analysed pressure and temperature quenched samples far from their thermodynamic stability field, the earlier experiments of Bolfan-Casanova et al. (2000) used infra-red (IR) spectroscopy to analyse for water content, while Inoue et al. (2010) used secondary ion mass spectroscopy (SIMS). It is possible that the samples lost their bound OH during quench, which would reduce the IR signal, but it is also possible that the SIMS analysis includes a contribution from micro-fluid inclusions. Whatever the reason, it is important to understand which is correct and to quantify H_2O solubility in perovskite.

We have, therefore, used first principles methods to calculate water partitioning between pure Mg-endmember perovskite and ringwoodite under mantle conditions. We find a partition coefficient of 13 at 1500 K and 10 at 2000 K. These are slightly lower, but still very similar to those found by Inoue et al. (2010). We also found that water strongly prefers perovskite over periclase (again under Fe-free conditions). We suggest, therefore, that the solubility of water in perovskite may indeed be as high as 1000 ppm. This figure results if we accept the partition coefficients between olivine, wadsleyite, ringwoodite and perovskite to be 6:30:15:1 (Inoue et al., 2010; Chen et al., 2002) and assume a maximum water storage capacity of 3.3 wt%, as determined by Inoue et al. (1995).

Because of its important geophysical implications, the incorporation of hydrogen into mantle minerals has been addressed employing computer simulations by several authors. Wright and Catlow (1994) studied the structure and energetics of OH defects in olivine using empirical potentials; Haiber et al. (1997) used first-principles molecular dynamics to study the dynamics of interstitial protons in the α, β and γ polymorphs of Mg_2SiO_4. Brodholt and Refson (2000)

* Corresponding author. Tel.: +34 91 3348994; fax: +34 91 372 0623.
** Corresponding author. Tel.: +44 2 76792622; fax: +44 2073887614.
E-mail addresses: Eduardo.Hernandez@csic.es (E.R. Hernández), D.Alfe@ucl.ac.uk (D. Alfè), J.Brodholt@ucl.ac.uk (J. Brodholt).

0012-821X/$ - see front matter © 2013 Elsevier B.V. All rights reserved.
http://dx.doi.org/10.1016/j.epsl.2013.01.005

used density functional theory to study hydrogen as an interstitial impurity and in interaction with cation vacancies in forsterite; they showed that the presence of hydrogen could promote the formation of cation vacancies, and this in turn could result in hydrolytic weakening. Braithwaite et al. (2003) used empirical potentials, quantum-mechanics/molecular-mechanics embedding methods and periodic electronic structure calculations to study the structure, energetics and vibrational frequencies of hydroxyl defects in forsterite. They found that hydroxyl ions were most likely to bind to cation vacancies forming neutral defects. Walker et al. (2006) later extended that study to cover also the cases of wadsleyite and ringwoodite. A review of the simulation work on hydrogen in mantle-forming minerals can be found in Wright (2006). More recent studies include those of Verma and Karki (2009), Panero (2010), and Umemoto et al. (2011). Verma and Karki (2009) have reported an extensive first principles study of both native and protonated defects in Mg_2SiO_4 polymorphs up to pressures of 30 GPa. Using the same methodology, Panero (2010) concluded that hydrogen would be most likely found in ringwoodite bound to cation vacancies; in particular, this study reported that the most abundant hydrogen-containing defect should be the Mg vacancy saturated by two protons, followed by the Si vacancy, containing four protons, and, less abundant, a substitutional Mg cation at a Si vacancy, saturated by two protons. Recently Li et al. (2011) calculated the elastic constants of H bearing olivine, wadsleyite and ringwoodite. They found that the bulk modulus of ringwoodite was unusually sensitive to water content, and suggested that $d\ln V_s/d\ln V_p$ could be used as a discriminator for water content in the transition zone.

The structure of this paper is as follows: in Section 2 we review our computational procedure, and derive an approximate expression for the partition coefficient. In Section 3 we present our results, starting with an evaluation of the ringwoodite to perovskite plus periclase phase boundary; this is a necessary prerequisite to evaluate the hydrogen partition coefficient at the relevant coexistence conditions. We then discuss the structures of various relevant cation vacancy-hydrogen complexes, and present our estimation of the hydrogen partition coefficient. Finally, our conclusions and discussion are presented in Section 4.

2. Computational details

2.1. First principles calculations

Our calculations have been carried out using the VASP program (Kresse and Furthmüller, 1996), an efficient code that implements density functional theory using a plane-wave basis set, with a convenient charge-density extrapolation technique (Alfè, 1999) which speeds up the simulations by roughly a factor of two. The valence electron–ion interaction has been treated employing the Projector Augmented Wave (PAW) method of Blöchl (1994) as implemented in VASP (Kresse and Joubert, 1999). We retained the $3s^2$ electrons of Mg, the $3s^23p^2$ electrons of Si and $2s^22p^4$ electrons of O, as well as the $1s^1$ electron of H (when appropriate), in the valence. A plane-wave kinetic energy cutoff of 500 eV was employed in all calculations, and the exchange–correlation energy was accounted for with the Perdew–Wang GGA functional (Perdew and Wang, 1992).

In order to determine the ringwoodite to perovskite and periclase phase boundary at finite temperatures we have used the quasi-harmonic approximation to obtain the Helmholtz free energy of each phase at constant volume. This was done by determining the phonon density of states of each phase at a series of volumes. The phonon band structure and density of states were obtained using the program PHON (Alfè, 2009) in conjunction with VASP. From the phonon densities of states two different approximations can be obtained to the free energy, namely a quantum approximation, which results from considering the lattice vibrations as an ensemble of quantum harmonic oscillators, or a classical one. These approximations are equivalent at high temperatures, but can differ slightly in the limit of low temperature.

Protonated cation vacancies in ringwoodite were modelled in the conventional cubic unit cell, which contains 56 atoms (16 Mg, 8 Si, 32 O). Since we anticipated that in both ringwoodite and the perovskite structures protons would preferentially substitute at Mg vacancies (see e.g. Panero, 2010), we performed our calculations in a $2\times2\times1$ supercell of perovskite (a total of 80 atoms), thus containing the same number of Mg ions as the ringwoodite cell. Convergence tests indicated that a $3\times3\times4$ Monkhorst–Pack (1976) grid gave sufficiently converged values of total energy and pressure in the case of the perovskite structure, while for ringwoodite a $4\times4\times4$ grid was employed. Structural optimisations were carried out with a convergence criterium requiring the absolute value of the force components to be smaller than 0.03 eV/Å.

2.2. Partition coefficient

The main objective of the present study is to provide an estimate of the partition coefficient of protons between the ringwoodite and perovskite phases at pressure conditions relevant to their coexistence in the Earth's mantle. Let us denote by n_r and n_p the number of proton-containing cation vacancies, $V_X(H_n)$, in ringwoodite and the perovskite phases, respectively, where X=Mg or Si and $n=2$ (if X=Mg) or $n=4$ (if X=Si). The total number of $V_X(H_n)$ complexes, n_v, is fixed, which implies the constraint $n_r+n_p=n_v$. We will further impose the condition of thermodynamic equilibrium between ringwoodite and the perovskite and periclase phases; this being the case, we can assume that there will be the same number of ringwoodite unit cells as of perovskite, denoted by N. However, because of the stoichiometry difference between these materials, there will be twice as many Mg sites in the former as there are in the latter. With the further assumption that the number of vacancy–proton complexes is small compared to N, i.e. $n_v \ll N$, we can construct a simple statistical model to estimate the partition coefficient, n_p/n_r, as follows: let us denote by $G_P(n_P)$ the Gibbs free energy of the perovskite phase containing n_p $V_X(H_n)$ complexes. With the above assumptions, this free energy can be written as

$$G_p(n_p) = G_p^0(n_p) - TS_p^{Conf}(n_p), \tag{1}$$

where $G_p^0(n_p)$ is the Gibbs free energy of N unit cells of perovskite containing n_p isolated (i.e. not clustering) $V_X(H_n)$ complexes, and $S_p^{Conf}(n_p)$ is the configurational entropy associated with the different ways in which n_p $V_X(H_n)$ can be distributed among N lattice sites. This configurational entropy has the form

$$S_p^{Conf}(n_p) = k_B \ln \frac{N_X!}{(N_X-n_p)!n_p!}, \tag{2}$$

where N_X is the number of X cation sites in the crystal (which in the cases considered is equal to N except in the case of Mg sites in ringwoodite, where $N_X=2N$; see below), and k_B is Boltzmann's constant. The first term in Eq. (1) can be written as

$$G_p^0(n_p) = (N-n_p)F_p^0 + n_pF_p^f(V_X(H_n)) + n_pP\Delta V_p, \tag{3}$$

where it is assumed that $V_X(H_n)$ complexes remain sufficiently far apart from each other that their mutual interaction can be ignored. In Eq. (3) F_p^0 is the Helmholtz free energy per unit cell for the perfect perovskite phase, $F_p^f(V_X(H_n))$ is the free energy of formation of a single $V_X(H_n)$ complex, P is the external pressure,

and ΔV_p is the change in unit cell volume upon formation of the complex.

Likewise, the Gibbs free energy of N unit cells of ringwoodite (i.e. $2N$ Mg sites) containing n_r $V_X(H_n)$ complexes would, under the same set of simplifying assumptions, be written as

$$G_r(n_r) = G_r^0(n_r) - TS_r^{Conf}(n_r). \quad (4)$$

The only difference with respect to the case of the perovskite phase is the fact that in the case of ringwoodite, due to the different stoichiometry, there are twice as many Mg sites among which to distribute the $V_{Mg}(H_2)$ complexes, which affects the configurational entropy.

The total free energy of a system containing equal amounts of Mg_2SiO_4 ringwoodite (with n_r $V_X(H_n)$ complexes) and $MgSiO_3$ perovskite (with n_p $V_X(H_n)$ complexes), and MgO periclase, is thus $G_{tot}(n_r,n_p) = G_r(n_r) + G_p(n_p) + G_{pe}$. Under conditions of thermal equilibrium, the complexes will partition themselves among the different phases in such a way as to minimise the total free energy. If we assume that $V_X(H_n)$ do not form in periclase, which is trivially the case for $V_{Si}(H_4)$ complexes, we can estimate the partition coefficient of such complexes between ringwoodite and the perovskite phase by simultaneously minimising Eqs. (1) and (4). As will be discussed below, the assumption that $V_{Mg}(H_2)$ complexes do not form in periclase is not entirely justified, but their concentration should be some 90 times smaller than in the perovskite phase. Bearing in mind that the total number of $V_{MX}(H_n)$ complexes is fixed (which implies that variations in n_p must be of equal magnitude but opposite sign as variations in n_r), and using Stirling's approximation for the factorials in Eq. (2), we find, after some simple algebra, the following expression for the partition coefficient of $V_{Mg}(H_2)$ complexes

$$\frac{n_p}{n_r} = \frac{1}{2} e^{\Delta G^f_{rp}(V_{Mg})/k_B T}, \quad (5)$$

where $\Delta G^f_{rp}(V_{Mg}) = G^f_r[V_{Mg}(H_2)] - G^f_p[V_{Mg}(H_2)]$ is the difference of Gibbs free energies of formation of a $V_{Mg}(H_2)$ complex in ringwoodite and perovskite, respectively. So, in order to estimate the partition coefficient of protons within the set of simplifying assumptions listed above, we need to evaluate ΔG^f_{rp}. This free energy difference should, strictly speaking, include the vibrational contribution to the free energies, necessitating at least the use of the quasi-harmonic approximation. While this could be an interesting prospect for future developments, at the present time we assume that the vibrational contribution of the protons to the free energies will be similar for both phases, and hence the difference will be small relative to the static energy difference. In this case the Gibbs free energies reduce to enthalpies, which are simpler to evaluate. The partition coefficient for $V_{Si}(H_4)$ has the same expression as Eq. (5) but without the 1/2 factor on the rhs, as the number of Si sites per unit cell is the same in ringwoodite as it is in the perovskite phase, and substituting $\Delta G^f_{rp}(V_{Mg})$ for $\Delta G^f_{rp}(V_{Si})$.

3. Results

3.1. Ringwoodite to perovskite and periclase transition

In our derivation of an approximate expression for the partition coefficient between $MgSiO_3$ perovskite and ringwoodite it has been assumed that these phases are in thermodynamic equilibrium with each other. Our starting point must therefore be to determine the coexistence conditions of these phases. We should note that at low temperatures a phase boundary between ringwoodite and the perovskite phase plus periclase is not expected, as there exists another phase of $MgSiO_3$, akimotoite[1] that should have its stability field lying between those of ringwoodite and the perovskite phase. Ringwoodite, akimotoite and the perovskite phase (the latter two together with periclase) should coexist at a triple point, the temperature coordinate of which is not known precisely, but is expected to be close to 1500 K (Stixrude and Lithgow-Bertelloni, 2011). At higher temperatures ringwoodite transforms directly into the perovskite phase plus periclase. Nevertheless, for the sake of simplicity we have obviated the existence of akimotoite and calculate the coexistence conditions between ringwoodite and perovskite at zero temperature.

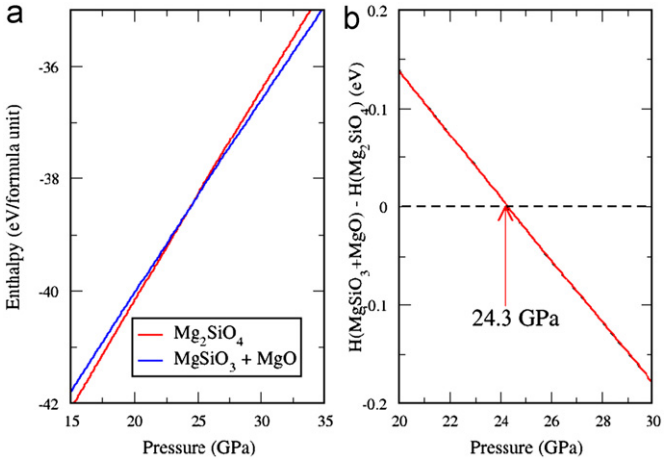

Fig. 1. Coexistence pressure of ringwoodite and perovskite plus periclase. Panel (a) shows a third-order polynomial fit of the enthalpies versus pressure, while panel (b) shows their difference, $\Delta H = H(MgSiO_3 + MgO) - H(Mg_2SiO_4)$; the point at which ΔH becomes zero marks the transition pressure (indicated by the arrow).

We have evaluated the enthalpy of the ringwoodite, perovskite and periclase phases at volumes roughly corresponding to 5 GPa pressure intervals ranging between 15 and 35 GPa. From the resulting enthalpies, displayed in Fig. 1 we can extract a coexistence pressure of 24.3 GPa. This value is in line with what is expected, both on the basis of experimental studies and previous theoretical calculations. For example, Yu et al. (2007) determined a transition pressure of 26.8 GPa on the basis of their GGA first principles calculations. Their value is only 2.5 GPa higher than ours; this could be due to a number of technical differences between their calculations and ours (a similar, but ultimately different exchange-correlation functional was used, and we employed the PAW method to describe core electrons, while they used norm-conserving pseudopotentials). It should also be borne in mind that the enthalpies (and more generally, free energies) cross at very small angles, as can be appreciated in Fig. 1, so small relative errors in the enthalpy of one phase with respect to the other can shift the coexistence pressure by several GPa. After evaluating the zero-temperature phase boundary, we proceeded to extend it into the finite temperature domain using the quasi-harmonic approximation to the free energy (see Section 2.1) for each of the phases considered. The quasi-harmonic free energies were evaluated at a series of volumes that corresponded to a pressure range of 0–30 GPa at zero temperature, at intervals of 2.5 GPa. A temperature grid ranging from 0 to 2500 K, with a temperature interval of 50 K was then constructed, and the Helmholtz free energy was evaluated for each phase on the resulting temperature–pressure grid. At a given temperature, the Helmholtz free energy of each phase was fitted to a third-order Birch–Murnaghan equation of state. From this the Gibbs

[1] $MgSiO_3$ akimotoite is rhombohedral, having the same structure as ilmenite.

free energy was then constructed, and the finite temperature phase boundary was located at each temperature in the grid by determining the pressure at which the Gibbs free energy of ringwoodite was found to be equal to the sum of Gibbs free energies of the perovskite plus periclase phases. Our resulting phase boundary is illustrated in Fig. 2. Two theoretical phase boundaries have been obtained, employing either the quantum or classical form of the quasi-harmonic approximation to the Helmholtz free energies. As can be seen in Fig. 2, though these deviate slightly from each other in the low temperature limit, they are in close agreement at higher temperatures.

The theoretical phase boundaries derived from this work are compared to experimentally determined ones in Fig. 2. Specifically, we have drawn straight lines with slopes adjusted to best fit the corresponding experimental data, as given in the original references. A first observation to be extracted from Fig. 2 is that our calculated phase boundaries fall within the range spanned by the experimental ones. The empirical phase boundaries share the characteristic of having a negative slope, a fact that our calculations correctly reproduce. The value of this slope, however, is difficult to determine precisely, and hence the scatter of experimental values should not be surprising. Early reports tended to give large negative slopes around -3 MPa/K; Ito and Takahashi (1989) report a value of -2.8 MPa/K, while Akaogi and Ito (1993) give it as -3 MPa/K and Shim et al. (2001) place it at -2.75 MPa/K. More recent studies tend to favour shallower slopes. For example Katsura et al. (2003) estimate the slope to be in the range -0.4 to -2 MPa/K; Fei et al. (2004) place it at -1.3 MPa/K and Litasov et al. (2005) report a value of -0.5 MPa/K. A very recent study by Ishii et al. (2011) favours a steeper value of -2 MPa/K. Our calculated value is -0.8 MPa/K ($\equiv 1236$ K/GPa), and is the same for both theoretical phase boundaries shown in Fig. 2 in the range of temperatures of geophysical interest (ca. 1600–2000 K). This value is close to the lower range of experimental slopes (Katsura et al., 2003; Fei et al., 2004; Litasov et al., 2005). The slope has also been calculated theoretically by Yu et al. (2007), who report values of -2.9 and -2.6 MPa/K when using a GGA and the LDA exchange-correlation functionals, respectively. As noted earlier, a number of technical differences between their computational procedure and ours could account for this discrepancy. Overall, from Fig. 2 we can conclude that our calculated phase boundary is in reasonable agreement with the reported experimental data.

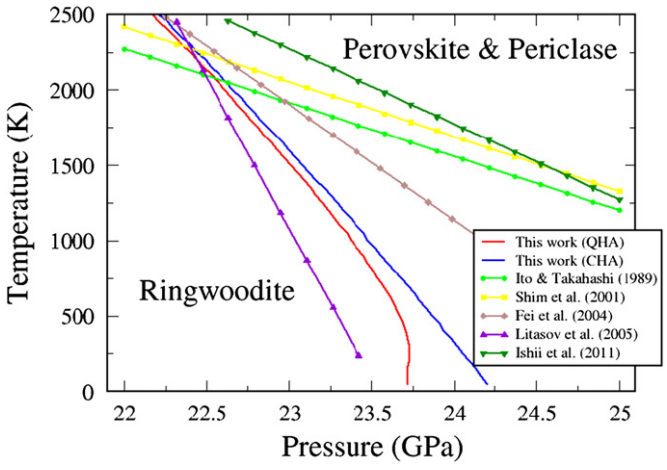

Fig. 2. Phase boundary between ringwoodite and perovskite plus periclase. Two theoretical curves are shown: the red line is obtained from quantum quasi-harmonic free energies, while the blue line is obtained using classical quasi-harmonic free energies. These phase boundaries deviate slightly from each other at low temperatures, but are in close agreement at higher temperatures, as expected. For comparison, boundaries inferred from experimental data are also shown. The light green line with circles is from Ito and Takahashi (1989); yellow line with squares Shim et al. (2001); brown with diamonds (Fei et al., 2004); purple with upward pointing triangles (Litasov et al., 2005), and dark green with downward pointing triangles (Ishii et al., 2011). (For interpretation of the references to colour in this figure caption, the reader is referred to the web version of this article.)

3.2. Cation-vacancy proton structures

We have considered the partitioning of two types of protonated cation-vacancy complexes, namely the $V_{Mg}(H_2)$ complex, in which two protons occupy the site of an Mg vacancy, and the $V_{Si}(H_4)$ complex, in which four protons are placed at the site of a Si vacancy. In ringwoodite Mg cations occupy octahedral sites, while in the perovskite phase they are found at cuboctahedral sites with a coordination of 12. Si cations, in contrast, occupy tetrahedral sites in ringwoodite, and octahedral ones in the perovskite phase. These differences will result in varying structures for their protonated vacancies, as we will see below. Let us first consider the structure of $V_{Mg}(H_2)$ in ringwoodite. In this structure we have found a minimum energy configuration in which the two protons lie along the O–O edges of the oxygen octahedron containing the vacancy. Each proton is bound to one of the oxygens on the octahedron edge, at a distance slightly under 1.1 Å that varies very little with pressure. The nearest non-bonded oxygen to the proton lies at a distance of 1.57 Å at 15 GPa, a distance that reduces to 1.45 Å upon increasing the pressure to 35 GPa. The O$-$H$\cdots$H angle remains fairly constant with pressure at 160°. Thus the incorporation of two protons into the void of the V_{Mg} results in the formation of two hydrogen-bonded bridges that partially saturate the Mg–O bonds broken by the creation of the vacancy. This structure corresponds to that labelled as H_2a by Li et al. (2009), and to the structures reported by Blanchard et al. (2005, 2009) for the $V_{Mg}(H_2)$ complex, and is illustrated in the upper left panel of Fig. 3.

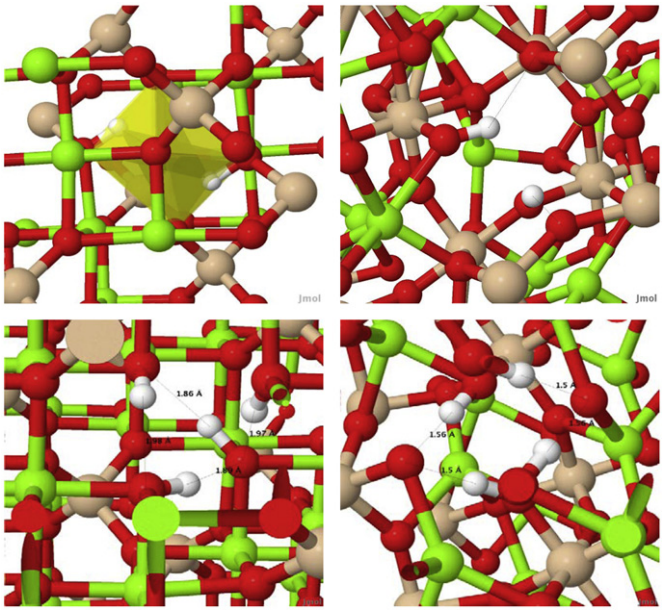

Fig. 3. Configurations of the most stable $V_{Mg}(H_2)$ and $V_{Si}(H_4)$ complexes found in ringwoodite and perovskite. Protons are shown as small white spheres; oxygen, magnesium and silicon atoms are shown as red, green and brown spheres, respectively. The upper-left and right panels show the configurations of $V_{Mg}(H_2)$ found in ringwoodite and perovskite, respectively, at 15 GPa. The octahedral vacancy volume in which the protons are accommodated in ringwoodite is highlighted in yellow. Likewise, the lower left and right panels show the configurations of $V_{Si}(H_4)$ in ringwoodite and perovskite, respectively. In some cases hydrogen bonds have been indicated by thin dotted lines. Figures have been created using J mol (an open-source Java viewer for chemical structures in 3D). (For interpretation of the references to colour in this figure caption, the reader is referred to the web version of this article.)

For the $V_{Mg}(H_2)$ complex in the perovskite phase the most stable configuration we have found follows the same general principles as that found in ringwoodite, although adapting to the different structures of the V_{Mg} in perovskite. We find an O–H bond distance close to 1.1 Å, decreasing slightly with pressure, an O···H distance of 1.65 Å, again reducing slightly with pressure, and a somewhat smaller O–H···H bond angle that ranges between 146° and 156° depending on its orientation. The structure we have found to be most stable is illustrated in the upper right panel of Fig. 3.

Concerning the structure of the $V_{Si}(H_4)$ complex in ringwoodite, there appears to be some controversy in the literature: Blanchard et al. (2009) report a structure in which the protons lie along the edges of the oxygen tetrahedron surrounding the vacancy as their most stable structure, while Li et al. (2009) claim that the most stable configuration has the protons pointing towards the V_{Si}. This latter configuration appears to be rather strange, as intuitively one would expect a high repulsion between protons in this arrangement. Indeed we have not been able to reproduce the finding reported by Li et al., and the structure we obtain as most stable (shown in the lower left panel of Fig. 3) corresponds to that reported by Blanchard and coworkers, being nearly 1 eV more stable than the structure of Li et al. at 15 GPa. We cannot rule out the possibility that this trend may be reversed at lower pressures, though this seems unlikely given the large energy difference we find. In the range of pressures considered here we have always found the structure of Blanchard et al. to be the most stable one.

The structure of the $V_{Si}(H_4)$ complex in perovskite that we have found most stable among those that we have tried is best understood as two equivalent pairs of protons. Each proton in the pair saturates an oxygen atom of the octahedron, and forms a hydrogen bond with one of the two unsaturated oxygen atoms that remain in the defective octahedron, in such a way that both protons in the pair form hydrogen bridges to the same unsaturated oxygen. This structure is shown in the lower right panel of Fig. 3.

We have also considered the possibility of having $V_{Mg}(H_2)$ complexes in periclase. In contrast to what happens in both ringwoodite and the perovskite phase, where the structure of the Mg vacancy is such that it allows for the formation of hydrogen bonds contributing to the overall stabilisation of the structure, the more compact configuration of the Mg vacancy in periclase appears to preclude their formation in this phase. In Fig. 4 we represent the most stable structure we have found for the $V_{Mg}(H_2)$ complex. It can be appreciated that the protons are forced to lie in a linear configuration, bonded to oxygen atoms in opposite vertices of the Mg octahedron containing the vacancy, by the presence of nearby cations. This linear configuration, with the two protons pointing towards the Mg vacant site, is energetically unfavourable, particularly at high pressures. Indeed, the energy involved in forming a $V_{Mg}(H_2)$ complex in periclase is 0.58 eV higher than in the perovskite phase at a pressure of 15 GPa, and this difference increases rapidly with pressure. Given these results, we can estimate, using the same arguments as employed in Section 2.2, that there would be 90 times more $V_{Mg}(H_2)$ complexes in perovskite than in periclase at the coexistence pressure and 1500 K.

Finally, we should stress that the catalogue of vacancy–proton complexes that we have contemplated in this work does not exhaust all the possibilities. For example, a complex in which a Mg cation occupies a Si lattice site, with two protons then entering into the Mg vacancy thus created would be a possible candidate. Such a complex has been studied by Blanchard et al. (2009), who concluded that its formation in ringwoodite was less energetically viable than that of either the $V_{Mg}(H_2)$ or $V_{Si}(H_4)$ complexes. Further possibilities exist, but it is to be expected that the cases we have considered here are the most representative ones, and that other possible mechanisms of hydrogen storage in these minerals would be of minor importance in comparison.

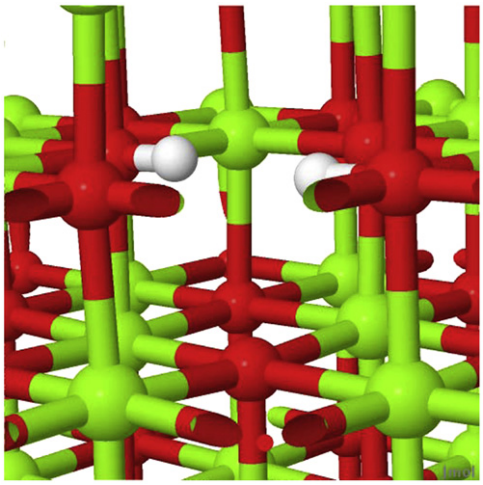

Fig. 4. Configuration of the most stable $V_{Mg}(H_2)$ complex found in periclase. Protons are shown as small white spheres; oxygen and magnesium atoms are shown as red and green spheres, respectively. Figure generated using J mol (an open-source Java viewer for chemical structures in 3D). (For interpretation of the references to colour in this figure caption, the reader is referred to the web version of this article.)

3.3. Hydrogen partitioning

As stated in Section 2.2, in this work we estimate the partitioning of hydrogen between ringwoodite and the perovskite phases assuming that the vibrational contribution to free energy differences is small. Thus the formation free energy difference appearing in Eq. (5) reduces to a difference of enthalpies of formation:

$$\Delta G^f_{rp} \simeq H^f_r[V_{Mg}(H_2)] - H^f_p[V_{Mg}(H_2)]. \quad (6)$$

Rather than attempting to evaluate each enthalpy of formation independently and then taking the difference, it is computationally more convenient to evaluate directly the enthalpy difference. This can be done by evaluating the following expression:

$$\Delta H^f_{rp} = (H_r[V_{Mg}(H_2)] - H_r) - (H_p[V_{Mg}(H_2)] - H_p) \quad (7)$$

where $H_{r(p)}[V_{Mg}(H_2)]$ is the enthalpy of a ringwoodite (or perovskite) supercell containing a single $V_{Mg}(H_2)$ complex, while $H_{r(p)}$ is that of the corresponding system without defect. Eq. (7) can be evaluated either at constant pressure, in which case the volume of the systems containing the vacancy complex must be carefully adjusted so as to retain a consistent, constant pressure for all phases, or at constant volume, using the same volume for both the perfect and defective system, in which case it reduces to a simple energy difference. It is easy to see that these two seemingly different approaches must give similar results; this is because the difference between both methods is, to leading order, proportional to the inverse of the bulk modulus of the materials involved, and therefore small. We have done the calculation both ways and verified that these alternative procedures lead to essentially equivalent results. Invariably, the creation of a $V_{Mg}(H_2)$ complex results in a pressure reduction if the calculation is performed at constant volume; this is so both for ringwoodite and the perovskite phases, and the pressure reduction can vary between 0.5 and 1 GPa, with the larger value corresponding to external pressures of 35 GPa. On the other hand, the creation of

a $V_{Si}(H_4)$ at constant volume increases the pressure by as much as 2.5 GPa in both phases. So, in order to evaluate Eq. (7) at a constant common pressure for all terms, we have fitted each term to a pressure polynomial, and then used those fits to calculate ΔH^f_{rp}. In Fig. 5 we display our estimated values for $\Delta H^f_{rp}[V_{Mg}(H_2)]$ and $\Delta H^f_{rp}[V_{Si}(H_4)]$ versus pressure, calculated using both second- and third-order pressure polynomial expansions for each of the terms in Eq. (7). As can be seen, the results obtained are not very sensitive to the order of the polynomials employed. It can also be appreciated in Fig. 5 that the value of $\Delta H^f_{rp}[V_{Mg}(H_2)]$ is rather insensitive to pressure, remaining close to avalue of -0.25 eV in the whole pressure range considered in this study. The negative sign indicates that the creation of $V_{Mg}(H_2)$ complexes is more favourable in ringwoodite. $\Delta H^f_{rp}[V_{Si}(H_4)]$ displays a slightly more marked pressure dependence, varying from -0.54 eV at 15 GPa to -0.6 eV at 35 GPa. Again the negative sign is indicative of the fact that these complexes will form more easily in ringwoodite than in the perovskite phase.

With the previous results in mind, we can now proceed to evaluate the partition coefficient Eq. (5) for both complexes. In the spirit of the approximations that allowed us to derive Eq. (5), we will assume that the processes underlying the partition of $V_{Mg}(H_2)$ and $V_{Si}(H_4)$ are mutually independent. In Fig. 6 we display the partition coefficients evaluated from Eq. (5) at our previously estimated coexistence pressure of 24.3 GPa (see Section 3.1), as a function of temperature. As seen in the figure, we obtain, for $V_{Mg}(H_2)$, a partition coefficient of 0.076 at 1500 K, increasing to 0.12 at 2000 K, while for $[V_{Si}(H_4)]$ the values are 0.016 and 0.045 at the same temperatures. Recently Inoue et al. (2010) have reported an experimental partition coefficient of $1/15=0.067$ at temperatures of 1673 and 1873 K. It should be understood that their partition coefficient is a global one, naturally incorporating all the relevant hydrogen inclusion mechanisms, while in our case we have only considered two. Even so, the agreement we obtain with their result is rather good, which we take as an indication that, in spite of its simplicity, our partition model accounts for the essential physico-chemical effects at play in these systems.

4. Discussion

In this work we have employed first principles total energy calculations to estimate the partition coefficient of hydrogen between Mg_2SiO_4 ringwoodite and $MgSiO_3$ perovskite at their predicted coexistence conditions. Our calculated partition coefficient is smaller than, but similar to that obtained experimentally by Inoue et al. (2010), but very different from the one reported by Bolfan-Casanova et al. (2000). The reasons for this marked disagreement between these two experimental determinations of the partition coefficient remain as yet unexplained. Both measurements followed similar experimental procedures, involving synthesis of samples at high pressures and temperatures followed by quenching to ambient conditions for subsequent analysis. Other than the fact that the samples employed by Bolfan-Casanova et al. (2000) were Fe-free, while those used by Inoue et al. (2010) contained some Fe, the main difference between these experiments were the techniques employed to quantify the amount of hydrogen present in the recovered minerals: Bolfan-Casanova et al. (2000) used IR spectroscopy, while Inoue et al. (2010) employed SIMS. This, however, is probably not the cause of the discrepancy, since Murakami et al. (2002) employed both IR spectroscopy and SIMS to determine the water content in their samples, obtaining consistent results. In view of the good agreement between our estimated partition coefficient and that measured by Inoue et al. (2010), it is unlikely that the presence of Fe in their samples could account for the difference with the results of Bolfan-Casanova et al. (2000), as our calculations were performed on Fe-free minerals. It seems, therefore, obvious that further experimental studies will be needed before the question of how much hydrogen can the perovskite structure accommodate is satisfactorily resolved.

As noted above, our estimated partition coefficient is slightly smaller than that determined by Inoue et al. (2010) (10–13 compared to 15). There are a number of reasons which may explain this difference: our results are on the Fe-free system, and we ignore the vibrational contribution to the free energies, accounting for temperature only through the configurational terms. Our model also assumes that water concentrations are

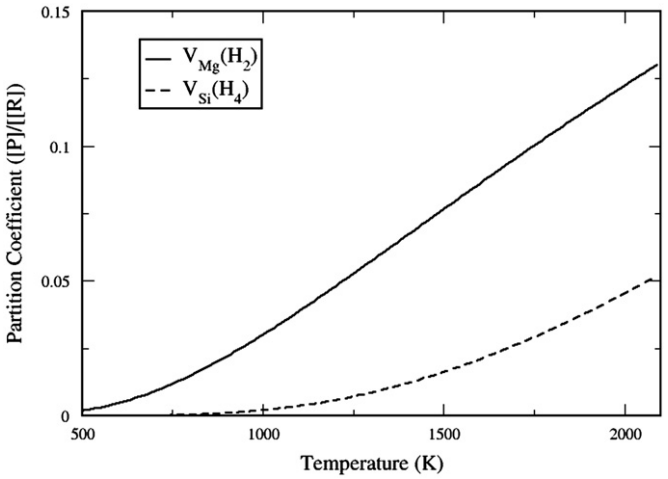

Fig. 6. Partition coefficient for $V_{Mg}(H_2)$ and $[V_{Si}(H_4)]$ complexes evaluated from Eq. (5) at the calculated coexistence pressure of 24.3 GPa (see Fig. 1).

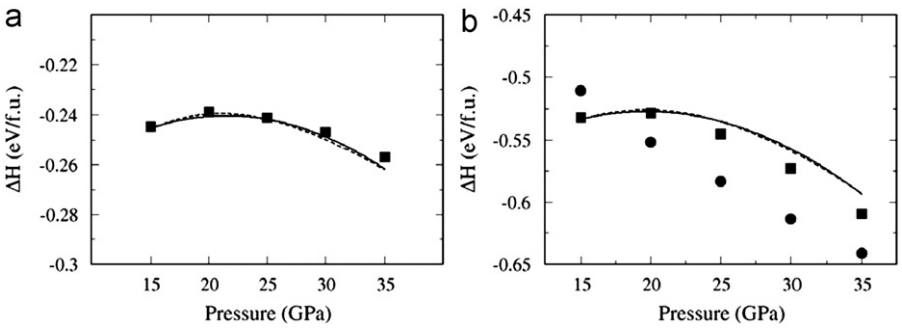

Fig. 5. Formation enthalpy differences for vacancy-proton complexes. Panel (a) shows the formation enthalpy difference for the $V_{Mg}(H_2)$ complex between ringwoodite and perovskite. The continuous and dashed lines are enthalpy differences evaluated at constant pressure and fitted to a second or third order polynomial in pressure (see text); the filled squares are values obtained from total energies at constant volume. Panel (b) shows the same information for the $V_{Si}(H_4)$ complex; additionally, filled circles give the formation enthalpy difference for the $V_{Mg}(H_2)$ between perovskite and periclase.

sufficiently low that interactions between protons on different vacancy sites are negligible. Finally, there may be other mechanisms for water incorporation that we did not consider, such as Mg and two protons substituting for Si (Panero, 2010). Further refinement of our calculations by improving on these approximations could potentially improve the observed agreement with the experimental results, but in the absence of more detailed knowledge of the contributing mechanisms of water uptake in ringwoodite and perovskite, such refinements are unlikely to result in a quantitative agreement. Nevertheless, the level of accord between the experimental data of Inoue et al. (2010) and our results is, we believe, indicative of the fact that our model captures the essential features of the process of water partitioning between these minerals.

Our results support the claim that perovskite is able to take up substantial amounts of water into its structure, perhaps as much as 1000 ppm or more. However, Inoue et al. (2010) also used their partition coefficients to suggest that the lower mantle should contain significantly less water than the upper mantle and transition zone. For instance, assuming 0.2 wt% water in wadsleyite, they used their partition coefficients to estimate that the lower mantle should contain only 0.007 wt% water. However, this is based on chemical equilibrium between the transition zone and lower mantle. Since even water diffusion is likely to be much slower than convection, chemical equilibrium will not be achieved. Instead, these partition coefficients show that as long as the upper mantle and transition zone contain less than about 0.1 wt% (1000 ppm) water, then the lower mantle should contain that amount as well.

Acknowledgements

The authors would like to thank Dr. M. Ammann and Prof. D. Dobson for useful discussions. E.R.H. thanks the Leverhulme Trust for the concession of a Leverhulme Visiting Professorship to UCL, during which this work was carried out, and the Spanish Ministry of Science and Innovation, for funding this research through Grant FIS2009-12721-C04-03. Our calculations were performed in the UCL ISD Research Computing cluster Legion.

References

Akaogi, M., Ito, E., 1993. Refinement of enthalpy measurement of $MgSiO_3$ perovskite and negative pressure–temperature slopes for perovskite-forming reactions. Geophys. Res. Lett. 20, 1839.

Alfè, D., 1999. Ab initio molecular dynamics, a simple algorithm for charge extrapolation. Comput. Phys. Commun. 118, 31–33.

Alfè, D., 2009. Phon: a program to calculate phonons using the small displacement method. Comput. Phys. Commun. 180 (12), 2622–2633.

Bell, D.R., Rossman, G.R., 1992. Water in Earth's mantle: the role of nominally anhydrous minerals. Science 255 (5050), 1391–1397.

Blanchard, M., Balan, E., Wright, K., 2009. Incorporation of water in Fe-free ringwoodite: a first-principles study. Am. Miner. 94 (1), 83–89.

Blanchard, M., Wright, K., Gale, J.D., 2005. A computer simulation study of oh defects in Mg_2SiO_4 and Mg_2GeO_4 spinels. Phys. Chem. Miner. 32 (8–9), 585–593.

Blöchl, P.E., 1994. Projector augmented-wave method. Phys. Rev. B 50, 17953–17979.

Bolfan-Casanova, N., Keppler, H., Rubie, D.C., 2000. Water partitioning between nominally anhydrous minerals in the $MgO–SiO_2–H_2O$ system up to 24 GPa: implications for the distribution of water in the Earth's mantle. Earth Planet. Sci. Lett. 182, 209–221.

Bolfan-Casanova, N., Mackwell, S., Keppler, H., McCammon, C., Rubie, D., 2002. Pressure dependence of h solubility in magnesiowustite up to 25 GPa: Implications for the storage of water in the Earth's lower mantle. Geophys. Res. Lett. 29 1449 (1–4).

Bolfan-Casanova, N., 2005. Water in the Earth's mantle. Mineral. Mag. 69 (3), 229–257.

Braithwaite, J.S., Wright, K., Catlow, C.R.A., 2003. A theoretical study of the energetics and ir frequencies of hydroxyl defects in forsterite. J. Geophys. Res.—Solid Earth 108 (1–9), 2284.

Brodholt, J., Refson, K., 2000. An ab initio study of hydrogen in forsterite and a possible mechanism for hydrolytic weakening. J. Geophys. Res.—Solid Earth 105 (B8), 18977–18982.

Chen, J., Inoue, T., Yurimoto, H., Weidner, D.J., 2002. Effect of water on olivine–wadsleyite phase boundary in the $(Mg, Fe)_2SiO_4$ system. Geophys. Res. Lett. 29, 1875.

Fei, Y., Orman, J.V., Li, J., van Westrenen, W., Sanloup, C., Minarik, W., Hirose, K., Komabayashi, T., Walter, M., Funakoshi, K.-I., 2004. Experimentally determined postspinel transformation boundary in Mg_2SiO_4 using MgO as an internal pressure standard and its geophysical implications. J. Geophys. Res. 109 (B2), B02305.

Haiber, M., Ballone, P., Parrinello, M., 1997. Structure and dynamics of protonated Mg_2SiO_4: An ab-initio molecular dynamics study. Am. Mineral. 82 (9–10), 913–922.

Inoue, T., Yurimoto, H., Kudoh, Y., 1995. Hydrous modified spinel, $Mg_{1.75}SiH_{0.5}O_4$: a new water reservoir in the mantle transition region. Geophys. Res. Lett. 22, 117–120.

Inoue, T., Wada, T., Sasaki, R., Yurimoto, H., 2010. Water partitioning in the Earth's mantle. Phys. Earth Planet. Inter. 183, 245–251.

Ishii, T., Kojitani, H., Akaogi, M., 2011. Post-spinel transitions in pyrolite and Mg_2SiO_4 and akimotoite–perovskite transition in $MgSiO_3$: precise comparison by high-pressure high-temperature experiments with multi-sample cell technique. Earth Planet. Sci. Lett. 309 (3–4), 185–197.

Ito, E., Takahashi, E., 1989. Postspinel transformations in the system $Mg_2SiO_4–Fe_2SiO_4$ and some geophysical implications. J. Geophys. Res. 94, 10637.

Katsura, T., Yamada, H., Shinmei, T., Kubo, A., Ono, S., Kanzaki, M., Yoneda, A., Walter, M.J., Ito, E., Urakawa, S., Funakoshi, K., Utsumi, W., 2003. Post-spinel transition in Mg_2SiO_4 determined by high p-t in situ x-ray diffractometry. Phys. Earth Planet. Inter. 136 (1–2), 11–24.

Kohlstedt, D.L., Keppler, H., Rubie, D.C., 1996. Solubility of water in the α, β and γ phases of $(Fe, Mg)_2SiO_4$. Contrib. Mineral. Petrol. 123, 345–357.

Kresse, G., Furthmüller, J., 1996. Efficient iterative schemes for *ab initio* total-energy calculations using a plane-wave basis set. Phys. Rev. B 54, 11169–11186.

Kresse, G., Joubert, D., 1999. From ultrasoft pseudopotentials to the projector augmented-wave method. Phys. Rev. B 59, 1758–1775.

Li, L., Weidner, D.J., Brodholt, J., Alfè, D., 2011. Prospecting for water in the transition zone: dln(Vs)/dln(Vp). Phys. Earth Planet. Inter. 189 (1–2), 117–120.

Li, L., Brodholt, J., Alfè, D., 2009. Structure and elasticity of hydrous ringwoodite: a first principle investigation. Phys. Earth Planet. Inter. 177 (3–4), 103–115.

Litasov, K., Ohtani, E., Langenhorst, F., Yurimoto, H., Kubo, T., Kondo, T., 2003. Water solubility in Mg-perovskites and water storage capacity in the lower mantle. Earth Planet. Sci. Lett. 211, 189–203.

Litasov, K., Ohtani, E., Sano, A., Suzuki, A., Funakoshi, K., 2005. In situ x-ray diffraction study of post-spinel transformation in a peridotite mantle: implication for the 660-km discontinuity. Earth Planet. Sci. Lett. 238 (3–4), 311–328.

Monkhorst, H.J., Pack, J.D., 1976. Special points for Brillouin-zone integrations. Phys. Rev. B 13, 5188–5192.

Murakami, M., Hirose, K., Yurimoto, H., Nakashima, S., Takafuji, N., 2002. Water in the Earth's lower mantle. Science 295, 1885–1887.

Panero, W.R., 2010. First principles determination of the structure and elasticity of hydrous ringwoodite. J. Geophys. Res. 115 (B3), B03203.

Perdew, J.P., Wang, Y., 1992. Accurate and simple analytic representation of the electron-gas correlation energy. Phys. Rev. B 45, 13244–13249.

Shim, S.-H., Duffy, T.S., Shen, G., 2001. The post-spinel transformation in Mg_2SiO_4 and its relation to the 660-km seismic discontinuity. Nature 411, 571–574.

Smyth, J.R., 1994. A crystallographic model for hydrous wadsleyite (β-Mg_2SiO_4): An ocean in the Earth's interior?. Am. Miner. 79, 1021–1024.

Stixrude, L., Lithgow-Bertelloni, C., 2011. Thermodynamics of mantle minerals—ii. Phase equilibria. Geophys. J. Int. 184 (January (3)), 1180–1213.

Umemoto, K., Wentzcovitch, R.M., Hirschmann, M.M., Kohlstedt, D.L., Withers, A.C., 2011. A first-principles investigation of hydrous defects and ir frequencies in forsterite: the case for Si vacancies. Am. Miner. 96 (10), 1475–1479.

Verma, A.K., Karki, B.B., 2009. Ab initio investigations of native and protonic point defects in Mg_2SiO_4 polymorphs under high pressure. Earth Planet. Sci. Lett. 285 (1–2), 140–149.

Wright, K., Catlow, C.R.A., 1994. A computer-simulation study of (OH) defects in olivine. Phys. Chem. Miner. 20 (7), 515–518.

Walker, A., Demouchy, S., Wright, K., 2006. Computer modelling of the energies and vibrational properties of hydroxyl groups in α- and β-Mg_2SiO_4. Eu. J. Miner. 18, 529–543.

Wright, K., 2006. Atomistic models of –OH defects in nominally anhydrous minerals. Rev. Miner. Geochem. 62, 67–83.

Yu, Y.G., Wentzcovitch, R.M., Tsuchiya, T., Umemoto, K., Weidner, D.J., 2007. First principles investigation of the postspinel transition in Mg_2SiO_4. Geophys. Res. Lett. 34 (10), L10306.